

# UNSUPERVISED IMAGE SEGMENTATION BASED ON THE MULTI-RESOLUTION INTEGRATION OF ADAPTIVE LOCAL TEXTURE DESCRIPTORS

Dana E. Ilea, Paul F. Whelan and Ovidiu Ghita

*Centre for Image Processing & Analysis (CIPA), Dublin City University, Glasnevin, Dublin 9, Ireland*

**Keywords:** Texture Segmentation, Multi-resolution Integration, Image Orientation, Texture Distribution.

**Abstract:** The major aim of this paper consists of a comprehensive quantitative evaluation of adaptive texture descriptors when integrated into an unsupervised image segmentation framework. The techniques involved in this evaluation are: the standard and rotation invariant Local Binary Pattern (LBP) operators, multi-channel texture decomposition based on Gabor filters and a recently proposed technique that analyses the distribution of dominant image orientations at both micro and macro levels. The motivation to investigate these texture analysis approaches is twofold: (a) they evaluate the texture information at micro-level in small neighborhoods and (b) the distributions of the local features calculated from texture units describe the texture at macro-level. This adaptive scenario facilitates the integration of the texture descriptors into an unsupervised clustering based segmentation scheme that embeds a multi-resolution approach. The conducted experiments evaluate the performance of these techniques and also analyse the influence of important parameters (such as scale, frequency and orientation) upon the segmentation results.

## 1 INTRODUCTION

Texture-based image segmentation represents a major field of research in the area of computer vision that has been intensively investigated for more than three decades. This has been motivated by the fact that the robust detection of texture primitives in digital images plays a key role in the identification of the constituent image regions. Taking into consideration the large spectrum of applications based on texture analysis, an impressive number of approaches has been published in the computer vision literature. As indicated in several reviews on texture-based segmentation (Tuceryan and Jain, 1998; Materka and Strzelecki, 1998) the existent techniques can be classified into four major categories: statistical, model-based, signal processing and structural. From these approaches most attention received the statistical and signal processing texture extraction methods.

Statistical methods are based on the evaluation of the spatial distributions and relationships between the pixel intensities in the image. Relevant statistical texture analysis techniques include the autocorrelation function (Haralick, 1979), texture

energy features (Laws, 1980), grey-level co-occurrence matrices (Haralick, 1979) and Local Binary Patterns (Ojala and Pietikainen, 1999). Based on the studies detailed in relevant papers focused on statistical texture analysis it can be concluded that these methods return adequate results when applied to synthetic images, but their performance is limited when applied to complex textured images.

To address some of the limitations associated with standard statistical texture analysis techniques, a non-parametric approach that analyses the texture at micro-level based on the calculation of the Local Binary Patterns (LBP) has been introduced by Ojala and Pietikainen, 1999. This approach attempts to decompose the texture into small units where the texture features are represented by the distribution of the LBP values. In (Ojala et al, 2002) the authors extended the initial LBP approach to address its sensitivity to rotation by introducing a new multi-resolution rotational invariant LBP texture descriptor whose performance was evaluated on standard texture databases.

The signal processing methods represent another important category of texture analysis techniques. These techniques were developed as a consequence of the psychophysical investigations that indicated

that the human brain performs a frequency analysis of the image perceived by the retina. Building on this concept, the signal processing techniques formulate the texture extraction in terms of the frequency information associated with the texture primitives present in digital images. Representative methods that belong to this category are: spatial domain filtering, Fourier analysis, Gabor filtering and Wavelet analysis. Among these signal processing methods, the approach that involves filtering an image with a bank of Gabor filters has gained the largest interest from the vision researchers (Bovik et al, 1990; Jain and Farrokhnia, 1991; Hofmann et al, 1998, Randen and Husoy, 1999). This approach implements a multi-channel texture decomposition and it is achieved by filtering the input image with 2D Gabor filter banks. (Bovik et al, 1990) used quadrature Gabor filters to segment images defined by oriented textures. The main conclusion resulting from their investigation is that the spectral difference sampled by narrow band filters provides sufficient information for texture discrimination. (Jain and Farrokhnia, 1991) followed a similar approach and developed a multi-channel Gabor filtering technique that was applied for image segmentation. In their paper, each filtered image was subjected to a non-linear transform and the energy was calculated within a pre-defined window around each pixel in the image. The energy features were afterwards clustered using a standard algorithm to obtain the segmented image. This approach was further advanced by (Randen and Husoy, 1999) while noting that filtering the image with a bank of Gabor filters or filters derived from Wavelet transform is computationally intensive. In their paper they proposed a new methodology to compute optimised filters for texture discrimination that requires a reduced number of filters than the standard implementation developed by Jain and Farrokhnia. A different segmentation strategy is proposed by (Hofmann et al, 1998) where the texture segmentation is formulated as a data clustering problem. In their approach the dissimilarities between pairs of textured regions are computed from a multi-scale Gabor filtered image representation. The resulting unsupervised segmentation scheme was successfully applied on both Brodatz textures and natural images.

Recently a novel hybrid statistical-structural approach was proposed where the texture is described in terms of the distribution of edge orientations calculated at micro and macro-level for all pixels in the image (Ilea et al, 2008; Ghita et al, 2008). The quantitative evaluations were conducted

on standard texture databases and the results indicated that the local image orientation based descriptor has a high discriminative power in the context of texture classification. In this study we will investigate its discrimination when applied to the unsupervised segmentation of complex textural arrangements.

The unsupervised segmentation process is in particular challenging since the texture attributes are not uniformly distributed within image areas defined by similar objects and often the strength of the texture can vary considerably from image to image. In addition to this, complications added by the uneven illumination, perspective and scale distortions make the process of identifying the homogeneous image regions with similar texture characteristics extremely difficult. The quantitative evaluation of the texture extraction techniques investigated in this paper was carried out using a segmentation framework similar to the one proposed in (Ilea and Whelan, 2009). The selection of this clustering-based segmentation technique for texture segmentation is justified as it provides an attractive platform for generalization and it also performs a global data optimization.

The selection of the texture analysis techniques evaluated in this study (the Local Binary Pattern Operators, texture decomposition using Gabor filtering and local orientation-based texture descriptor) is also justified, as they allow an adaptive texture analysis (at micro and macro-level) when integrated into an unsupervised clustering approach. The adaptive approach considered in this paper provides a robust scenario for texture segmentation and together with a comprehensive numerical evaluation of the above mentioned methods it represents a contribution of this paper in the study of texture features segmentation.

This paper is organised as follows. Section 2 briefly introduces the texture analysis methods investigated in this study and discusses the motivation behind their selection. Section 3 describes the experimental setup and presents the numerical evaluation followed by a discussion of the obtained results. Section 4 concludes the paper.

## 2 EVALUATED TEXTURE EXTRACTION METHODS

**The Standard LBP/C Operator** - The LBP operator (Ojala and Pietikainen, 1999) is a powerful texture descriptor as it analyses the texture at micro-

level, but at the same time the macro characteristics of texture are sampled by the distribution of the LBP values. The LBP texture unit is calculated by thresholding the values of the pixels in a  $3 \times 3$  neighbourhood with respect to the value of the central pixel, while the LBP value is calculated by multiplying the elements of the texture unit with binomial weights (that are powers of 2 with respect to the position of the pixels in the neighbourhood) and summing the result.

To further improve the robustness of the LBP operator and allow the sampling of the illumination offsets between different textures, the standard LBP operator is used in conjunction with the contrast operator,  $C$ . The contrast measure  $C$  is calculated as the difference between the average grey-level of the pixels with values 1 and the pixels with values 0 contained in the  $3 \times 3$  texture unit. The main advantage of analysing the texture using the distribution of LBP/ $C$  values is given by the fact that they can be used to discriminate textures in the input image regardless the region size. The distribution of the LBP/ $C$  values calculated over an image region represents the texture spectrum that can be defined as a joint histogram of size  $(256 + bins)$ , where the first 256 bins are required by the distribution of the LBP values and  $bins$  represents the number of bins employed to sample the contrast measure. Based on the experiments performed by Ojala and Pietikainen, the best results are obtained when the contrast distribution is quantised into 4 to 16  $bins$ . The optimal selection of the number of bins is a difficult issue since for low values of  $bins$  the histogram will lack resolution, while for high values of  $bins$  the histogram will become sparse and unstable. Based on experimentation it has been demonstrated that a quantisation of the contrast measure in 8  $bins$  returns the best results.

**The Rotation Invariant LBP Operator ( $LBP^r$ )** - The standard LBP values calculated for each texture unit are sensitive to texture orientation. This is motivated by the fact that the elements of the texture unit uniquely encode the position of each pixel in the  $3 \times 3$  neighbourhood. To remove the sensitivity to rotation, the texture descriptor is calculated within a circular neighbourhood and the texture is evaluated in terms of uniformity. A uniform pattern is defined as the number of transitions between 0 and 1 in the LBP mask obtained after thresholding the pixels from the circular neighbourhood with the intensity value of the central pixel. In this way, the authors defined a pattern as uniform if the binary LBP pattern has maximum two transitions; otherwise the pattern is labelled as non-uniform. To improve its

discriminative power, the  $LBP^r$  value is complemented with the contrast measure that is calculated as the variance of the pixels situated in the LBP mask. For more details regarding the calculation of the LBP operators, the reader can refer to (Ojala and Pietikainen, 1999; Ojala et al, 2002).

**Texture Analysis using Gabor Filters** is an approach that implements a multi-channel texture decomposition and is achieved by filtering the input image with a two-dimensional (2D) Gabor filter bank that was introduced by (Daugman, 1988) and later applied to texture segmentation by (Jain and Farrokhnia, 1991). The 2D Gabor function that is used to implement the even-symmetric 2D discrete filters can be written as follows:

$$G_{\sigma, f, \varphi}(x, y) = \exp\left(-\frac{x'^2 + y'^2}{2\sigma^2}\right) \cos(2\pi f x' + \varphi) \quad (1)$$

In equation (1)  $x' = x \cos \theta + y \sin \theta$ ,  $y' = -x \sin \theta + y \cos \theta$ ,  $\sigma$  is the scale parameter of the Gabor filter,  $\theta$  is the orientation and  $f$  is the frequency parameter that controls the number of cycles of the cosine function within the envelope of the 2D Gaussian ( $\varphi$  is the phase offset and it is usually set to zero to implement 2D even-symmetric filters). The parameters of the Gabor filters are chosen to optimise the trade-off between spectral selectivity and the size of the bank of filters. Typically, the central frequencies are selected to be one octave apart and for each central frequency is constructed a set of filters corresponding to four ( $0^\circ$ ,  $45^\circ$ ,  $90^\circ$ ,  $135^\circ$ ) or six orientations ( $0^\circ$ ,  $30^\circ$ ,  $60^\circ$ ,  $90^\circ$ ,  $120^\circ$ ,  $150^\circ$ ).

**Texture Extraction using the Dominant Image Orientation at Micro and Macro-levels** is an approach defined in terms of the distribution of the dominant edge orientations at micro and macro-level and was introduced in (Ilea et al, 2008; Ghita et al, 2008). In this regard, the orientation for each pixel in the image is extracted using the partial derivatives of the Gaussian function ( $G$ ) while the main focus is the evaluation of the local dominant orientation.

An important parameter is the scale ( $\sigma$ ) of the Gaussian function and its role is to control the amount of noise reduction. After the calculation of the partial derivatives, the weak edge responses were eliminated by applying a non-maxima suppression procedure (Canny, 1986) and the edge orientation is calculated. As indicated in (Ilea et al, 2008), the problem of analysing the texture orientation at a given observation scale is not a straightforward task

as the orientation of textures may be isotropic at macro-level but having a strong orientation at micro-level. Therefore, we propose to evaluate the dominant orientation of the texture calculated at micro-level for all texture units that are defined as the local neighbourhood around each pixel in the image, while the distribution of the dominant orientations calculated for all texture units is employed to capture the dominant orientation of texture at macro-level.

In this implementation, the orientation of the texture is determined by constructing the histogram of orientations for all pixels in the local neighbourhood and the dominant orientation is selected as the dominant peak in the histogram as follows,

$$\begin{aligned}
 H_{\Theta}(x,y) &= \bigcup_{i \in D} h_{\Theta}(x,y,i), D \in [0, 2\pi] \\
 h_{\Theta}(x,y,i) &= \sum_{x-(w/2)}^{x+(w/2)} \sum_{y-(w/2)}^{y+(w/2)} \delta(\Theta(x,y),i) \\
 \delta(i,j) &= \begin{cases} 1 & i = j \\ 0 & i \neq j \end{cases} \\
 \Theta(x,y) &= \arctg \left[ \frac{G_y \circ f(x,y)}{G_x \circ f(x,y)} \right] \text{ and} \\
 \Theta_d &= \arg \max(H_{\Theta})
 \end{aligned} \tag{2}$$

In equations (2) and (3),  $\Theta$  is the local orientation, the symbol  $\circ$  defines the convolution operation,  $G_y = \partial G / \partial y$ ,  $G_x = \partial G / \partial x$ ,  $f(x,y)$  is the pixel value at position  $(x,y)$  in the original image,  $i$  is the orientation bin,  $D$  defines the orientation domain,  $H_{\Theta}(x,y)$  is the distribution of the local orientations calculated around pixels situated at positions  $(x,y)$  and  $\Theta_d$  is the dominant texture orientation in the neighbourhood  $w \times w$ . The dominant orientation at macro-level ( $H_{\Theta_d}$ ) is estimated by the distribution of the local dominant orientations that are determined over the region of interest as follows,

$$H_{\Theta_d} = \bigcup_{i \in D} \int_{\Gamma} \delta(\Theta_d^{w \times w}(x,y),i) d\Gamma \tag{4}$$

where  $\Gamma$  is the image domain. In equation (4) it should be noted that the texture orientation is sampled at a pre-defined observation scale that is controlled by the size of the neighbourhood  $w \times w$ .

The dominant orientation is not robust in sampling the difference between textures that are subjected to illumination variation. Thus, the local texture orientation is augmented with measures such

as local orientation coherence and contrast ( $C$ ) that are calculated in the local neighbourhood  $w \times w$  where the dominant orientation of the texture has been estimated. The contrast measure ( $C$ ) is sampled by the mean grey-scale value calculated in the  $w \times w$  neighbourhood and the orientation coherence ( $\Theta_c$ ) is calculated using the weighted standard deviation of the edge orientation of all the pixels in the neighbourhood  $w \times w$ .

### 3 EXPERIMENTS AND RESULTS

In this paper, we have modified the computational architecture of the segmentation framework proposed in (Ilea and Whelan, 2008) in order to provide a robust scenario for texture segmentation. The main steps of the proposed texture segmentation algorithm are illustrated in Figure 1. It is important to mention that the texture features are independently extracted from the luminance component of the input image to exclusively evaluate the texture information.

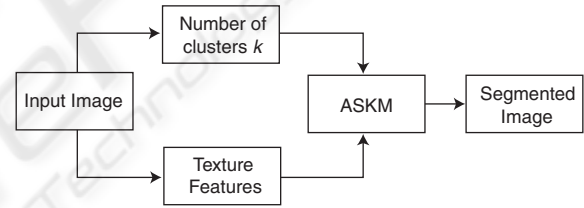


Figure 1: Overview of the texture segmentation algorithm.

The Adaptive Spatial K-means (ASKM) clustering is the main component of the segmentation method. The main idea behind ASKM is to minimise an objective function  $J_T$  based on the fitting between the local texture distributions calculated for each pixel in the texture image and global texture distributions calculated for each cluster as follows,

$$J_T = \sum_{x=1}^{width} \sum_{y=1}^{height} \left\{ \sum_{i=1}^k \min_{s \in \{3 \times 3, \dots, 25 \times 25\}} KS(H_T^{s \times s}(x,y), H_T^i) \right\} \tag{5}$$

In equation (5),  $k$  is the number of clusters,  $s \times s$  defines the size of the local window,  $H_T^{s \times s}(x,y)$  is the local texture distribution calculated for the pixel at position  $(x,y)$  and  $H_T^i$  is the texture distribution for the cluster with index  $i$  respectively. The number of clusters  $k$  is automatically calculated in conjunction with the number of textures in the image as indicated

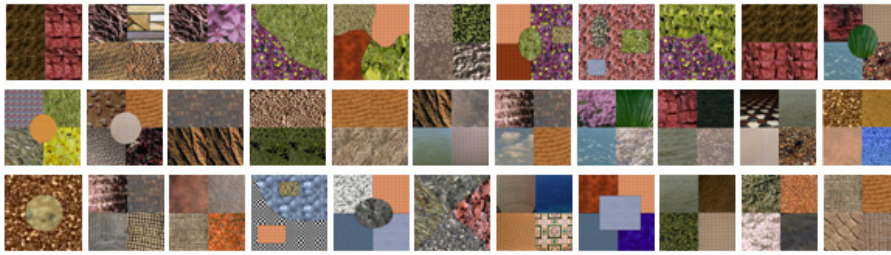


Figure 2: The database of 33 mosaic images used in our experiments.

in (Ilea and Whelan, 2008). The similarity between the local texture distribution and the global texture distribution of the clusters is evaluated using the Kolmogorov-Smirnov (*KS*) metric (Rubner et al, 2001). The fitting between the local texture distributions and global texture distributions of the clusters is performed adaptively for multiple window sizes in the interval  $[3 \times 3]$  to  $[25 \times 25]$ . While textures in the image are not uniform, the multi-resolution approach detailed in this paper offers an attractive scheme for texture segmentation as it allows the variation of the window size until the best fit between the global and local texture distributions is achieved.

**Experimental Setup** - Since the ground truth data associated with complex natural images is difficult to estimate and its extraction is highly influenced by the subjectivity of the human operator, the texture segmentation evaluation was performed on mosaic data where the ground truth is unambiguous. Therefore, the segmentation algorithm described in the previous section was applied to a database of 33 mosaic images (image size  $184 \times 184$ ) that were created by mixing complex textures from (VisTex 2000) and Photoshop databases. The mosaics used in these experiments consist of various texture arrangements that also include images where the borders between different regions are irregular. The suite of 33 mosaic images is depicted in Figure 2.

The quantitative measurements were carried out using the Probabilistic Rand Index (PR) (Unnikrishnan and Hebert, 2005) that measures the agreement between the segmented result and the ground truth data and takes values in the range  $[0, 1]$ . A higher PR value indicates a better match between the segmented result and the ground truth data. The PR Index is defined in the appendix of this paper. In this study, for every analysed texture analysis technique, the PR mean and standard deviation were computed for all images in the database. The construction of the texture vectors is illustrated in Figure 3. It can be noticed that the feature vectors are defined either by the LPB/C joint distributions or by the distributions calculated from

the responses obtained after filtering the image with the multi-channel filter bank (the intensity values of the filtered images were normalised in the interval  $[0, 255]$  so the size of the feature vector is  $256 \times$  number of filters in the filter bank). For the edge orientation-based technique, the texture vector is given by the joint distribution defined by the dominant orientation ( $\Theta_d$ ), the contrast (*C*) and the orientation coherence ( $\Theta_c$ ).

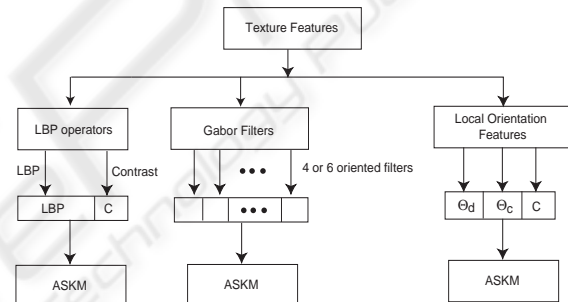


Figure 3: The calculation of the texture distributions.

### 3.1 Results Returned by the LBP Technique

The first set of tests evaluates the segmentation performance when using the standard Local Binary Pattern (LBP) and the rotation invariant  $LBP_{8,1}^{ri}$ ,  $LBP_{16,2}^{ri}$ ,  $LBP_{24,3}^{ri}$  texture descriptors. As indicated above, the experiments were performed on a database consisting of mosaic images and the numerical results are illustrated in Table 1 (the  $LBP_{p,R}^{ri}$  defines the rotation invariant LBP operator where *P* is the number of pixels in the LBP mask and *R* is the radius of the mask).

The results illustrated in Table 1 indicate that the LBP/C operator provides better discrimination in its standard form than the rotation invariant  $LBP_{8,1}^{ri}$ ,  $LBP_{16,2}^{ri}$ ,  $LBP_{24,3}^{ri}$  descriptors. The LBP/C operator returned the highest PR values for 21 out of 33 mosaic images, while the  $LBP_{8,1}^{ri}$  operator returned the lowest PR values for 13 images out of 33. The drop in segmentation accuracy for rotation invariant LBP descriptors indicates that the invariance to rotation, as expected, is attained at the expense of

the loss in discriminative power. This conclusion is justified since the LBP uniform patterns are not able to sample the directional characteristics of the texture.

Table 1: Quantitative results when the LBP/C texture descriptors were evaluated in the proposed segmentation framework.

| Method                               | PR <sub>mean</sub> | PR <sub>standard_deviation</sub> |
|--------------------------------------|--------------------|----------------------------------|
| LBP/C                                | 0.84               | 0.12                             |
| LBP <sub>8,1</sub> <sup>ri</sup> /C  | 0.80               | 0.11                             |
| LBP <sub>16,2</sub> <sup>ri</sup> /C | 0.82               | 0.09                             |
| LBP <sub>24,3</sub> <sup>ri</sup> /C | 0.82               | 0.12                             |

### 3.2 Results Returned by the Gabor Filtering Technique

In order to evaluate the multi-channel texture decomposition scheme based on Gabor filtering, the input image has been processed with a small bank of filters with four ( $0^\circ$ ,  $45^\circ$ ,  $90^\circ$ ,  $135^\circ$ ) and six ( $0^\circ$ ,  $30^\circ$ ,  $60^\circ$ ,  $90^\circ$ ,  $120^\circ$ ,  $150^\circ$ ) orientations. The central frequency and the scale parameters were also varied. The standard deviation (scale) parameter was set to the values 1.0, 2.0 and 3.0 respectively, while the central frequency parameter was varied by setting it to the following values  $1.5/2\pi$ ,  $2.0/2\pi$  and  $2.5/2\pi$ , respectively.

Table 2: Quantitative results when the Gabor filtering (GF) technique was evaluated in the proposed segmentation framework.

| Scale ( $\sigma$ ) | Method                       | PR <sub>mean</sub> | PR <sub>st_dev</sub> |
|--------------------|------------------------------|--------------------|----------------------|
| $\sigma = 1.0$     | GF $f = 1.5/2\pi$ , 4 angles | 0.46               | 0.24                 |
|                    | GF $f = 2.0/2\pi$ , 4 angles | 0.61               | 0.17                 |
|                    | GF $f = 2.5/2\pi$ , 4 angles | 0.81               | 0.12                 |
|                    | GF $f = 1.5/2\pi$ , 6 angles | 0.50               | 0.26                 |
|                    | GF $f = 2.0/2\pi$ , 6 angles | 0.62               | 0.18                 |
|                    | GF $f = 2.5/2\pi$ , 6 angles | 0.81               | 0.12                 |
| $\sigma = 2.0$     | GF $f = 1.5/2\pi$ , 4 angles | 0.65               | 0.17                 |
|                    | GF $f = 2.0/2\pi$ , 4 angles | 0.83               | 0.10                 |
|                    | GF $f = 2.5/2\pi$ , 4 angles | 0.85               | 0.08                 |
|                    | GF $f = 1.5/2\pi$ , 6 angles | 0.65               | 0.17                 |
|                    | GF $f = 2.0/2\pi$ , 6 angles | 0.84               | 0.09                 |
|                    | GF $f = 2.5/2\pi$ , 6 angles | 0.85               | 0.08                 |
| $\sigma = 3.0$     | GF $f = 1.5/2\pi$ , 4 angles | 0.78               | 0.13                 |
|                    | GF $f = 2.0/2\pi$ , 4 angles | 0.85               | 0.08                 |
|                    | GF $f = 2.5/2\pi$ , 4 angles | 0.85               | 0.11                 |
|                    | GF $f = 1.5/2\pi$ , 6 angles | 0.79               | 0.12                 |
|                    | GF $f = 2.0/2\pi$ , 6 angles | 0.84               | 0.08                 |
|                    | GF $f = 2.5/2\pi$ , 6 angles | 0.86               | 0.08                 |

### 3.3 Results Returned by the Local Orientation-based Texture Descriptor

In (Ilea et al, 2008; Ghita et al, 2008) a texture descriptor based on the evaluation of the dominant image orientation calculated at micro and macro-level was proposed. In this section, experimental results that quantify the performance of the image orientation based texture descriptor in the segmentation process are provided. For these experiments the value of the parameter  $\sigma$  (that sets the scale of the derivative of the Gaussian function) is set to 0.5 and 1.0. The experimental results illustrated in Table 3 indicate that the optimal results are obtained when the scale parameter  $\sigma$  is set to 0.5.

Table 3: Quantitative results for the local orientation based texture extraction technique when the window size is varied.

| Scale ( $\sigma$ ) | Window size    | PR <sub>mean</sub> | PR <sub>standard_deviation</sub> |
|--------------------|----------------|--------------------|----------------------------------|
| $\sigma = 0.5$     | $3 \times 3$   | 0.83               | 0.12                             |
|                    | $7 \times 7$   | 0.82               | 0.11                             |
|                    | $11 \times 11$ | 0.82               | 0.12                             |
| $\sigma = 1.0$     | $3 \times 3$   | 0.81               | 0.12                             |
|                    | $7 \times 7$   | 0.81               | 0.12                             |
|                    | $11 \times 11$ | 0.81               | 0.11                             |

There are two reasons behind the selection of this value for the  $\sigma$  parameter. The first is motivated by the fact that with the increase in the value of the scale parameter the edges derived from weak textures are eliminated and the second reason consists in the requirement to increase the size of the derivative of the Gaussian filters with the increase of the scale parameter  $\sigma$ . The feature vectors for the edge orientation technique are formed by the joint distributions (see Figure 3) constructed using the dominant orientation, the contrast and the orientation coherence. The experiments were conducted on the mosaic database when the size of the texture unit  $w \times w$  is varied. The experimental data shown in Table 3 indicates that optimal performance is obtained when the texture orientation is sampled in small texture units and these results are motivated by the fact that the texture orientation is best analysed at micro-level.

## 4 CONCLUSIONS

The aim of this paper was to evaluate the performance of a number of statistical and signal processing texture analysis techniques when applied to image segmentation. The techniques evaluated in this study are: the LBP/C operators, multi-channel texture decomposition based on Gabor filter banks and a recently proposed texture analysis technique based on the evaluation of the image orientation at micro and macro-level. The main novelty associated with this work resides in the evaluation of the analysed texture descriptors in a multi-resolution framework offered by the proposed texture segmentation algorithm and in the evaluation of the experimental results when the parameters associated with these techniques are varied. Our experiments show that the method based on texture decomposition using Gabor filters marginally outperformed the other analysed techniques. The experimental data reinforced the concept that texture is an important attribute of digital images and it also indicates that the local orientation is the dominant feature that provides the primary discrimination between textures.

## ACKNOWLEDGEMENTS

This work was funded in part by the HEA PRTLI IV National Biophotonics & Imaging Platform Ireland (NBIPI) and the Science Foundation Ireland (Research Frontiers Programme).

## REFERENCES

- Bovik, A. C., Clark, M., Geisler, W. S.: Multi-channel Texture Analysis Using Localized Spatial Filters. *IEEE Transactions on Pattern Analysis and Machine Intelligence*, Vol. 12, No. 1 (1990) 55-73
- Canny, J.: A Computational Approach to Edge Detection. *IEEE Transactions on Pattern Analysis and Machine Intelligence*, Vol. 8, No. 6 (1986) 679-698
- Daugman, J. G.: Complete Discrete 2D Gabor Transforms by Neural Networks for Image Analysis and Compression. *IEEE Transactions on Acoustics, Speech and Signal Processing*, Vol. 36, No. 7 (1988) 1169-1179
- Ghita, O., Whelan, P. F., Ilea, D. E.: Multi-resolution Texture Classification Based on Local Image Orientation. In *Proceedings of the 5<sup>th</sup> International Conference on Image Analysis and Recognition (ICIAR)*, Portugal (25-27 July, 2008) 688-696
- Haralick, R. M.: Statistical and Structural Approaches to Texture. In *Proceedings of the IEEE*, Vol. 67, No. 5 (1979) 786-804
- Hofmann, T., Puzicha, J., Buhmann, J. M.: Unsupervised Texture Segmentation in a Deterministic Annealing Framework. *IEEE Transactions on Pattern Analysis and Machine Intelligence*, Vol. 20, No. 8 (1998) 803-818
- Ilea, D. E., Ghita, O., Whelan, P. F.: Evaluation of Local Orientation for Texture Classification. In *Proceedings of the 3<sup>rd</sup> International Conference on Computer Vision Theory and Applications (VISAPP)*, Portugal (22 - 25 January 2008) 357-364
- Ilea, D. E., Whelan, P. F.: CTex - An Adaptive Unsupervised Segmentation Algorithm Based on Colour-Texture Coherence. *IEEE Transactions on Image Processing*, Vol. 17, No. 10 (2008) 1926-1939
- Jain, A. K., Farrokhnia, F.: Unsupervised Texture Segmentation Using Gabor Filters. *Pattern Recognition*, Vol. 24, No. 12 (1991) 1167-1186
- Laws, K. L.: Rapid Texture Identification. In *Proceedings of the SPIE Conference on Image Processing for Missile Guidance*, Vol. 238 (1980) 376-380
- Materka, A., Strzelecki M.: Texture Analysis Methods – A Review. Technical Report, University of Lodz, Cost B11 Report (1998)
- Ojala, T., Pietikainen, M.: Unsupervised Texture Segmentation Using Feature Distributions. *Pattern Recognition*, Vol. 32, No. 3 (1999) 477-486
- Ojala, T., Pietikainen, M., Maenpaa, T.: Multiresolution Grey-scale and Rotation Invariant Texture Classification with Local Binary Patterns. *IEEE Transactions on Pattern Analysis and Machine Intelligence*, Vol. 24, No. 7 (2002) 971-987
- Randen, T., Husoy, J. H.: Texture Segmentation Using Filters with Optimised Energy Separation. *IEEE Transactions on Image Processing*, Vol. 8, No. 4 (1999) 571-582
- Rubner, Y., Puzicha, J., Tomasi, C., Buhmann, J. M.: Empirical Evaluation of Dissimilarity Measures for Colour and Texture. *Computer Vision and Image Understanding*, Vol. 84, No. 1 (2001) 25-43
- Tuceryan, M., Jain, A. K.: *Texture Analysis*. In: Chen, C.H., Pau, L.F., Wang, P.S.P. (eds.): *Handbook of Pattern Recognition and Computer Vision*, World Scientific Publishing (1998)
- Vision Texture (VisTex) Database, Massachusetts Institute of Technology, MediaLab. <http://vismod.media.mit.edu/vismod/imagery/VisionTexture/vistex.html>
- Unnikrishnan, R., Hebert, M.: Measures of Similarity. In *Proceedings of IEEE Workshop on Computer Vision Applications*, Vol. 1 (2005) 394 – 394

## APPENDIX

The Probabilistic Rand index (PR) was proposed in (Unnikrishnan and Hebert, 2005) with the aim of obtaining a quantitative evaluation of the

segmentation result when compared to one or more ground truth (manual) segmentations. Let  $S_{test}$  be the segmented image that will be compared against the manually labelled set of ground truth images  $\{S_1, S_2, \dots, S_G\}$  (where  $G$  defines the total number of manually segmented images). The segmentation result is quantified as appropriate if it correctly identifies the pairwise relationships between the pixels as defined in the ground truth segmentations.

In other words, the pairwise labels  $l_i^{S_{test}}$  and  $l_j^{S_{test}}$  (corresponding to any pair of pixels  $x_i, x_j$  in the segmented image  $S_{test}$ ) are compared against the pairwise labels  $l_i^{S_g}$  and  $l_j^{S_g}$  in the ground truth segmentations and vice versa. Based on this principle, the PR index is defined as follows:

$$PR(S_{test}, \{S_{1..G}\}) = \frac{1}{\binom{N}{2}} \sum_{\substack{i,j \\ i \neq j}} [I(l_i^{S_{test}} = l_j^{S_{test}}) \cdot p_{ij} + I(l_i^{S_{test}} \neq l_j^{S_{test}}) \cdot (1 - p_{ij})] \quad (6)$$

In equation (6)  $N$  is the total number of pixels in the image,  $I(l_i^{S_{test}} = l_j^{S_{test}})$  denotes the probability that the pair of pixels  $x_i$  and  $x_j$  have the same label in  $S_{test}$  and  $p_{ij}$  represents the mean pixel pair relationship between the ground truth images.

$$p_{ij} = \frac{1}{G} \sum_{g=1}^G I(l_i^{S_g} = l_j^{S_g}) \quad (7)$$

The PR index takes values in the interval  $[0, 1]$  and a higher PR value indicates a better match between the segmented result and the ground truth data. The PR index takes the value 0 when there are no similarities between the segmented result and the set of manual segmentations and it takes the value 1 when all segmentations are identical.